Maximum attainable power density and wall load in tokamaks underlying reactor relevant constraints

K. Borrass
R. Buende

IPP 4/182 September 1979

MAX-PLANCK-INSTITUT FÜR PLASMAPHYSIK
8046 GARCHING BEI MÜNCHEN

MAX-PLANCK-INSTITUT FÜR PLASMAPHYSIK

GARCHING BEI MÜNCHEN

Maximum attainable power density and wall load in tokamaks underlying reactor relevant constraints

K. Borrass

R. Buende

IPP 4/182 September 1979

Die nachstehende Arbeit wurde im Rahmen des Vertrages zwischen dem Max-Planck-Institut für Plasmaphysik und der Europäischen Atomgemeinschaft über die Zusammenarbeit auf dem Gebiete der Plasmaphysik durchgeführt.

IPP 4/182

Maximum attainable power density and wall load in tokamaks underlying reactor relevant constraints

K. Borrass
R. Buende

September 1979

Abstract

The characteristic data of tokamaks optimized with respect to their power density or wall load are determined. Reactor relevant constraints are imposed, such as a fixed plant net power output, a fixed blanket thickness and the dependence of the maximum toroidal field on the geometry and conductor material. The impact of finite burn times is considered. Various scaling laws of the toroidal beta with the aspect ratio are discussed.

The analysis is performed analytically and numerically with the SISYFUS-T power plant model.

The systems with maximum power density or wall load are essentially completely characterized by their aspect ratio and the scaling of toroidal beta with the aspect ratio. They depend only weakly on the plant size, the absolute value of the maximum toroidal field and the factor of proportionality in the scaling laws for beta.

For the various assumptions on beta scaling the maximum typically occurs in the range $2 \lesssim A \lesssim 4.5$. The impact of finite burn times is modest. There is no essential difference between power density and wall load maximization. In the range $2 \lesssim A \lesssim 4.5$ the power density or wall load may deviate by roughly 50 % from its maximum value.

CONTENTS

1. INTRODUCTION

Fusion reactor studies during the past few years have greatly enhanced the trend to more compact systems. In this context "more compact" is often understood in the sense of higher power density or wall load. This trend is based on the assumption that the installation costs of a reactor are the lower the more compact the reactor is. However, one has to bear in mind that a reactor layout optimized with respect to its installation costs is not necessarily identical with a reactor layout which achieves minimum power production costs of a fusion power plant. A higher wall load probably requires more often replacement of the first wall, thus leading to longer outage times. These may even be prolonged by the compactness of the reactor. On the other hand, it cannot be excluded that systems with maximized power density or wall load at least approximate overall optimized designs. In any case they are natural prominences worth studying as points of reference for optimization studies.

Here we determine the characteristic data of tokamak plasmas which are optimized as to their power density or wall load. The position in parameter space where the respective maximum is reached obviously depends strongly on the constraints imposed on the system. Besides the plasma particle and energy balances, the essential constraints considered in this paper are a prescribed net power output, the relation between β_T and geometrical parameters, and the relation between the toroidal field and geometrical data or conductor material.

We proceed in two steps. The first part of the paper is an approximate analytic discussion giving a general overview and allowing easy comparison of different scaling laws of, for instance, β_T with A etc., which have still to be verified in future experiments.

The second part presents calculations with the SISYFUS-T fusion power plant model /5/ /6/ within which the above-mentioned constraints are incorporated. By means of these calculations the assumptions underlying the above analytic considerations are checked and more specific questions are handled for a variety of examples.

2. ANALYTIC TREATMENT

In this part we consider systems that are characterized by the following conditions:

a) They are pulsed with a burn time τ_b such that $\tau_b >> \tau_s, \tau_d$, where τ_s is the start-up time and τ_d the going-down time.

b) β_T is kept fixed by a controlled refuelling procedure.

c) The transport laws are such that the plasma burns in a stable manner.

d) The pulse duration is determined by wall impurity accumulation. α-particles are assumed not to accumulate.

Conditions a) to d) obviously select a representative class of systems. The same class of systems was studied in Ref. /1/, which we shall occasionally refer to. As was shown in Ref. /1/, the mean (time and volume-averaged) fusion power density can be approximated by

$$p_f \sim \bar{\beta}_T^{\,2} \; B_T^{\,4} \; \frac{\tau_b}{\tau_b + \tau_o} \qquad (1)$$

for these systems, where $\bar{\beta}_T$ is the volume-averaged toroidal beta, B_T the toroidal field on axis, τ_b the burn time and τ_o the idle time.

In Ref. /1/ τ_b was studied for the systems under consideration within the framework of a global particle and energy balance /2/. It depends on, among other parameters, $\bar{\beta}_T$, B_T, A, a or equivalently on $\bar{\beta}_T$, B_T, A, V, where A is the plasma aspect ratio, a the plasma minor radius and V the plasma volume. In a real system these parameters are no longer independent owing to additional constraints which further restrict the space of admitted parameters. p_f has to be maximized in this reduced parameter space. The following constraints have to be taken into account: $P_{e,net}$ = const, which means that p_f has to be maximized for a prescribed power output $P_{e,net}$. In a system with Q >> 1 this condition is approximately equivalent to

P_f = const, where P_f is now the mean fusion power /3/. Q >> 1 is given for systems characterized by a) to d). By definition one has

$$P_f = V \; p_f. \tag{2}$$

An additional constraint stems from the requirement that the toroidal field at the inner coil must not exceed a limiting value. This condition can be put in the form

$$B_T \; (1- \frac{f}{A})^{-1} \leq B_{max}, \tag{3}$$

where $f = 1 + \frac{\Delta}{a}$ and Δ is the distance between the plasma boundary and the inner coil. B_{max} is determined by either the critical field B_c of the respective superconductor material or the maximum admitted strain, which depends on the coil geometry in addition to the coil material /4/. From the more general result of Ref. /4/ the following simplified expression for B_{max} is obtained in the Appendix:

$$B_{max} = \min \; (B_c, \; k \; (A/V)^{1/6} \; \frac{1}{\sqrt{f} \; \sqrt{1-f/A}}). \tag{4}$$

For NbTi B_{max} is typically determined by the critical field B_c, whereas for Nb_3Sn the strain condition is generally more severe. The situation is made more complex by the fact that the coefficient k in eq. (4) depends on, for instance, the coil thickness. It is thus possible, for instance, to shift the threshold of the strain condition by readjusting the coil thickness. This scheme will be discussed in the context of the numerical treatment. To simplify the evaluation of eq. (4), we shall treat the cases

$$B_{max} = B_c \tag{5}$$

and

$$B_{max} = k \; (A/V)^{1/6} \; \frac{1}{\sqrt{f} \; \sqrt{1-f/A}} \tag{6}$$

as alternatives. This will be justified by the fact that the results differ only slightly for these two cases.

Finally, for each geometry there exists an upper limit for $\overline{\beta}_T$ resulting from equilibrium and stability considerations:

$$\overline{\beta}_T \leq C(A,....), \tag{7}$$

where .... indicates other parameters such as the eccentricity in the noncircular case, the safety factor q(a), etc. The A-dependence is assumed to be dominant. All concrete relations that will be discussed later are of the form

$$\overline{\beta}_T \leq C'/A^m \tag{8}$$

or

$$\overline{\beta}_P \leq C''/A^{m-2}. \tag{9}$$

As noted above, one has $\Delta = a_s + d + \frac{b}{2}$, where a_s is the plasma wall distance, d the blanket thickness and b the coil thickness. Typically $d >> a_s + \frac{b}{2}$. Furthermore, the blanket thickness for a given blanket design is essentially independent of the plasma size. In what follows, we shall thus assume

$$\Delta = \text{const} \tag{10}$$

as an additional constraint.

For convenience we now write eqs. (3) and (8) in the form

$$B_T = z_1 \; B_{max} \; (1-f/A) = z_1 \; B_T^o \tag{11}$$

and

$$\overline{\beta}_T = z_2 \; C'/A^m = z_2 \; \overline{\beta}_T^o \; , \tag{12}$$

with $0 \leq z_1, z_2 \leq 1$. The values $z_1, z_2 = 1$ correspond to equality in eqs. (3) and (8). Eliminating B_T and $\overline{\beta}_T$ from eq. (1) by means of eqs. (11) and (12), we get the following expression for p_f:

$$p_f \sim z_1^4 \, z_2^2 / A^{2m} \, (1-f/a)^4 \left[(A/V)^{1/6} \frac{}{\sqrt{f}\ \sqrt{1-f/A}} \right]^{4\sigma} \frac{\tau_b}{\tau_b + \tau_o} \qquad \sigma = 0,1, \qquad (13)$$

where $\sigma = 0$ characterizes the critical field condition and $\sigma = 1$ characterizes the strain condition for the maximum field at the superconductor.

As is obvious from eq. (13), in the case $\tau_b \gg \tau_o$ p_f has the maximum value if $z_1 = z_2 = 1$, i.e. if equality holds in eqs. (3) and (8).

In the case of finite burn time $\tau_b = \tau_b \, (A, V, \overline{\beta}_T, B_T, \ldots) =$ $= \tau_b \, (A, V, z_2 \, \overline{\beta}_T^o, \, z_1 B_T^o, \ldots)$. In Ref. /1/ it was demonstrated for trapped particle transport that τ_b monotonically increases with $\overline{\beta}_T$ and $B_T, A, a, \ldots$ being kept fixed. From the results presented there it is easy to conclude that the same holds for $A, V, \ldots$ being kept fixed. Hence $\tau_b \, (A, V, z_2 \, \overline{\beta}_T^o, \, z_1 B_T^o, \ldots) \leq \tau_b \, (A, V, \overline{\beta}_T^o, \, B_T^o, \ldots)$ and consequently with eq. (13) p_f again has a maximum value if equality holds in eqs. (3) and (8). The situation may be different if other transport laws prevail and must be discussed specifically. In what follows we shall assume as an example that the above situation is given in the case of finite burn time and shall take equality in eqs. (3) and (8) throughout. We now have

$$p_f \sim 1/A^{2m} \, (1-f/A)^4 \left[(A/V)^{2/3} \frac{1}{f^2 \, (1-f/A)^2} \right]^{\sigma} \frac{\tau_b}{\tau_b + \tau_o} \qquad (14)$$

$$\sigma = 0,1,$$

where p_f is a function of $A, V, , \ldots$. To find the system where p_f has its maximum value, P_f and Δ being kept fixed, one has to solve

$$\frac{\partial \, p_f}{\partial \, A} \Big|_{P_f, \Delta} = 0. \qquad (15)$$

If $\tau_b \ll \tau_o$ and $B_{max} = B_c$, p_f as given by eq. (13) no longer depends on V. Hence p_f does not depend on P_f in this limit and the expression for p_f as given by eq. (14) can immediately be inserted in eq. (15). In general, it is difficult to get a manageable expression for p_f as a function of A, P_f, Δ,... . This problem can be circumvented in the following way. Differentiating the identity $P_f = P_f\,(A,V\,(A,P_f))$ with respect to A yields

$$0 = \frac{\partial P_f}{\partial A}\bigg|_{V,\Delta} + \frac{\partial P_f}{\partial V}\bigg|_{A,\Delta} \cdot \frac{\partial V}{\partial A}\bigg|_{P_f,\,\Delta}. \tag{16}$$

From eq. (2) we have

$$0 = \frac{\partial V}{\partial A}\bigg|_{P_f,\Delta} \cdot\; p_f + V\,\frac{\partial p_f}{\partial A}\bigg|_{P_f,\Delta}\,. \tag{17}$$

Hence from eqs. (16) and (17), again using eq. (2), it follows that

$$\frac{\partial p_f}{\partial A}\bigg|_{V,\Delta} = \frac{1}{p_f}\,\frac{\partial P_f}{\partial V}\bigg|_{A,\Delta}\,\frac{\partial p_f}{\partial A}\bigg|_{P_f,\Delta}. \tag{18}$$

From eq. (18) we conclude that eq. (15) is equivalent to

$$\frac{\partial p_f}{\partial A}\bigg|_{V,\Delta} = 0. \tag{19}$$

We now evaluate eq. (19) using the expression (14) for p_f. At first the limit $\tau_b >> \tau_o$ will be considered. Some qualitative conclusions will then be drawn as to the impact of finite burn times.

Inserting eq. (14) in eq. (19) results in an equation for the values A, V, Δ for which p_f has a maximum. By elementary methods one gets

$$A_m = \begin{cases} f+2/3\;\; \dfrac{2f+1}{m} & \sigma = 0, \\[2ex] f+\dfrac{2(2f+1)}{3(2m-2/(3f))} & \sigma = 1, \end{cases} \tag{20}$$

where A_m is the aspect ratio for which, for given Δ and V, and hence f, p_f has its maximum value. The typical value of f is $f \approx 1.4 - 1.8$.

In Table 1 some values of A_m are summarized for f = 1.6, σ = 0,1 and m = 1,3/2,2.

Table 1

	m = 1	m = 3/2	m = 2
σ = 0	A_m = 4.40 $\bar{\beta}_T$ = 0.036	A_m = 3.47 $\bar{\beta}_T$ = 0.025	A_m = 3.00 $\bar{\beta}_T$ = 0.018
σ = 1	A_m = 3.37 $\bar{\beta}_T$ = 0.047	A_m = 2.68 $\bar{\beta}_T$ = 0.036	A_m = 2.38 $\bar{\beta}_T$ = 0.028

The result as given by eq. (20) is remarkably simple insofar as A_m does not depend on the coefficients of proportionality in eqs. (6) and (8). Furthermore, it depends on Δ and V only through f, this quantity varying only slightly with the size of the system. A_m always increases with increasing f and decreases with increasing m. The values of A_m are roughly 20 % lower in the case σ =1 (strain condition) than in the case σ = 0 (critical field condition). If compared with typical values of A in present reactor designs A_m is rather high if σ = 0.

In Table 1 the values of $\bar{\beta}_T$ are added that correspond to A_m if C'' is set equal to 1 in eq. (9). Then m=1,3/2,2 corresponds to $\bar{\beta}_P \lesssim A, \sqrt{A}, 1$. It was assumed in all cases that q = 2.5. In all cases the values for $\bar{\beta}_T$ are rather low and would not exceed 10 % even if some elongation effects were taken into account. This illustrates that $\bar{\beta}_T$ alone is not a good measure of the power density obtainable in a tokamak.

In the case of finite burn times the factor $\tau_b/(\tau_b+\tau_o)$ becomes relevant in eq. (14). In the case under consideration it is a monotonically increasing function of A. From the explicit form of p_f as given by eq. (14) it is obvious that V and hence f being fixed, it shifts A_m as given by eq. (20) to higher values. On the other hand $\tau_b/(\tau_b+\tau_o) < 1$ requires an enhanced volume to achieve the same power output. An increase of V makes f decrease. As noted above this shifts A_m to lower values. As we shall find numerically both effects compensate in practice.

We now return to the problem of maximizing the wall load q_w for fixed Δ and P_f. By definition one has

$$P_f = O \cdot q_w, \tag{21}$$

where O is the plasma surface. (For simplicity we assume $a_s \ll a$.) With $V \sim O^{3/2}/A^{1/2}$ we get from eq. (14) for q_w as a function of A, O, Δ

$$q_w \sim \frac{A^\sigma}{A^{2m+1/2} f^{2\sigma}} (1-f/A)^{4-2\sigma} \qquad \sigma = 0,1. \tag{22}$$

By complete analogy we can now deduce from eqs. (21) and (22) that solving equation $\frac{\partial q_w}{\partial A}/_{P_f,\Delta}=0$ is equivalent to solving

$$\frac{\partial q_w}{\partial A}/_{O,\Delta} = 0. \tag{23}$$

Inserting eq. (22) in eq. (23) yields by elementary methods

$$A'_m = \begin{cases} f + \dfrac{1+f}{m+1/4} & \sigma = 0, \\ f + \dfrac{1+f}{2(m+1/4)-1/f} & \sigma = 1, \end{cases} \tag{24}$$

where A'_m is now the aspect ratio such that q_w for given Δ and O and hence f takes its maximum.

Table 2 gives some values for $f=1.6, \sigma = 0,1$, $m = 1, 3/2, 2$. The values of A'_m as given by eq. (24) are slightly lower (typically less then 15 %) than the values A_m given by eq. (20).

Table 2

	m = 1	m = 3/2	m = 2
$\sigma = 0$	$A'_m = 3.68$	$A'_m = 3.09$	$A'_m = 2.76$
$\sigma = 1$	$A'_m = 2.99$	$A'_m = 2.50$	$A'_m = 2.27$

It thus makes no essential difference whether the system is optimized with respect to its power density or wall load.

3. NUMERICAL TREATMENT

In this part we discuss some calculations with the SISYFUS-TE code. It allows the computation of p_f and q_w for given $P_{e,net}$, Δ, A without making any of the simplifying assumptions of the foregoing section. Hence, besides checking these assumptions, we can study the behaviour of p_f and q_w in the vicinity of the maximum as well as the quantitative impact of finite burn times for specific cases. In addition, some calculations with α-particle accumulation were performed where the simple expression for p_f as given by eq. (1) is no longer valid because of fuel displacement effects.

A description of the SISYFUS-TE code (Simulation model for systematic analyses of fusion power plants, T ≙ tokamak; E ≙ energy balance), which was developed at IPP Garching, is given in /6/. The main features of this code are: a one-dimensional time-dependent plasma model including control of β by refuelling during the burn phase and the possibility of taking into account impurities from the wall and either accumulation or anomalous outward diffusion of α-particles. In this application the option of the trapped-ion mode is used. The blanket calculations assume stainless steel as structure and wall material and liquid lithium as coolant and breeding material. The blanket geometry is fixed at a constant thickness of 0.75 m with 6 % structure material yielding a tritium breeding ratio of 1.25. The heat transport system is without an intermediate loop. The energy conversion system is a steam turbine cycle with an upper steam temperature of 500 ^{o}C resulting in a gross thermal efficiency of 39.8 %. For each combination of input parameters the minor plasma radius is adjusted iteratively so that the required net electric power output $P_{e,net}$ of the plant is achieved; in this case this output was fixed at $P_{e,net}$ = 1500 MW_e. The number of toroidal coils is determined within the model of the toroidal magnets according to a given ripple coefficient for the magnetic field. In addition, this model

affords two options for calculating the maximum magnetic field at the superconductor. With the first option this field is calculated according to the kind of conductor material and cooling temperature. The thickness of the constant-tension D-shaped coils is adjusted so that a given value for the strain in the conductor is utilized but not exceeded. By means of this adjustment it is possible to realize the maximum magnetic field given by the conductor material and the cooling temperature. This case corresponds to the case $\sigma = 0$ in the foregoing section. With the second option the thickness of the toroidal coils is fixed so that it may happen that the maximum magnetic field has to be lower because of the strain limit ($\sigma = 1$).

In Fig. 1 the plasma power density is represented as a function of the aspect ratio under the condition of the material's limit (solid line) and the strain limit (dashed lines with the designations of different toroidal coil thicknesses D). These curves are based on the following assumptions: anomalous outward diffusion of α-particles, no impurity accumulation within the plasma (impurity reflux coefficient $\gamma = 0$), $\beta_p = A$ ($m = 1$), superconductor material NbTi with Cu as stabilizer material, maximum temperature of the conductor 5 K, yielding a maximum admissible field of 8.46 T if the thickness D can be adjusted under the condition of a strain limit of $\varepsilon = 0.1$ %. Along the solid line in Fig. 1 the coil thickness D slightly increases with increasing aspect ratio. At $A = 3.85$ this thickness is $D = 1.1$ m, at $A = 4.5$ it is $D = 1.13$ and at $A = 5$ it is $D = 1.15$ m.

The strain limitation becomes effective when a maximum coil thickness D is fixed at a value which is lower than that necessary to utilize the material's capability at $\varepsilon = 0.1$ %. In this case the maximum magnetic field at the superconductor was adequately reduced, thus yielding a reduction of the magnetic field at the plasma centre and consequently of the power density in the plasma. The results are represented by the dashed lines in Fig. 1. A maximum value of $D = 1.1$ m (upper curve) allows utilization of the superconductor material's capability in the range of $A \lesssim 3.85$. Higher aspect ratios yield a reduction in power density, and lower values for the coil thickness D yield additional reductions.

As regards looking for optimum aspect ratios, it is interesting to know from Fig. 1 that these values in the cases of material and of stress limitation differ only slightly, and that in addition - in agreement with the analytical result - the maximum power densities at stress limitation occur nearly at the same aspect ratio. It is thus sufficient to base the following considerations on the material's limitation of the magnetic field.

In Figs. 2 and 3 the plasma power density and the wall load are represented as functions of the aspect ratio on the assumption of anomalous outward diffusion of the α-particles. Each of the figures contains three triples of lines, corresponding to $\beta_p = A$, $\beta_p = \sqrt{A}$ and $\beta_p = 1$ respectively. Each triple itself comprises a solid line, a dashed line and a dashed-and-dotted line. The solid line represents the clean case ($\gamma = 0$). The dashed line refers to an impurity reflux coefficient of $\gamma = 1.25 \times 10^{-4}$ and the dashed-and-dotted line to $\gamma = 5 \times 10^{-4}$ /6/.

In Fig. 2 the steps from the solid lines (infinite burn time) to the dashed lines and to the dashed-and-dotted lines (finite burn times) show that the power density (cycle time averaged) decreases with increasing γ in all cases of β_p scaling. This is due to the fact that the burn time decreases with increasing γ thus giving the idle time τ_o an increasing percentage of the total cycle time. The aspect ratio for maximum power density shifts only slightly to lower values with increasing impurity contamination.

Figure 3 shows that the wall load (burn time averaged) increases with increasing impurity contamination of the plasma. The maximum wall load values occur at lower aspect ratios. Nevertheless, the curves are sufficiently flat so that a 20 % deviation of the aspect ratio from its optimum value is relatively meaningless.

In Figs. 2 and 3 anomalous outward diffusion of the α-particles was assumed. The real behaviour of α-particles in a reactor plasma is not yet known. As an alternative the complete accumulation of the α-particles within the plasma was therefore considered, too. The power density and wall loading in both cases are compared in Figs. 4 and 5

respectively at $\gamma = 0$, the scaling of β_p being varied again. The reference case of anomalous outward diffusion of α-particles is given by the solid lines identical with those of the corresponding Figs. 1 and 2. In Figs. 4 and 5 the dashed lines refer to complete accumulation of α-particles.

The comparison between the different assumptions on α-particle behaviour shows that the aspect ratios that are optimum with respect to the power density (Fig. 4) shift to lower values in either case of β_p scaling by less than 20 %. As the curves with complete α-particle accumulation are flatter, deviations from the optimum aspect ratio are less effective than in the other case. In addition, the influence of the choice of A again decreases with the steps from $\beta_p = A$ to $\beta_p = \sqrt{A}$ and further to $\beta_p = 1$. Nearly the same is true when considering the influence of the α-particle behaviour on the wall load (Fig. 5).

Some of the foregoing calculations admit direct comparison with the analytical results. The values of A_m and A_m' as predicted by eq. (20) and eq. (24) for $\sigma = 0$ are marked by vertical lines in Figs. 2 and 3. In applying eqs. (20) and (24) the values for f were taken from the numerical calculation at the maximum point. There is complete agreement between the analytical and numerical results. As pointed out earlier, f varies only slightly in the range considered.

The dashed lines in Fig. 1 correspond to $\sigma = 1$. The values of A_m as predicted by eq. (20) for $\sigma = 1$ are marked in an analogous way. The somewhat worse agreement is likely to be caused by the approximations made in deriving eq. (5) of the Appendix.

4. CONCLUSION

The power density p_f and wall loading q_w of tokamaks underlying reactor relevant constraints have been studied. The constraints considered are:

- a burn cycle with β_T controlled at a prescribed value
- fixed plant net power output
- fixed blanket thickness
- a prescribed scaling of $\overline{\beta}_T$ of the form $\overline{\beta}_T \sim 1/A^m$
- a maximum value for the toroidal field at the coil, given by the critical field or a strain limitation.

The discussion is performed analytically and numerically.

From the analytic discussion it follows that the aspect ratio for which the power density or wall load attains its maximum value depends on the system's parameters only through $f = 1 + \Delta/a$. f varies only in a narrow range. The systems with maximum power density or wall load are thus essentially characterized by their aspect ratio, independently of the net electric power output (that is the size), the absolute values of β_T and the absolute value of B_{max}.

There is not much difference between the optimum aspect ratio with respect to power density or wall load. Whether B_{max} is determined by the critical field or the maximum allowable strain is also of minor importance.

The main impact stems from the scaling of $\bar{\beta}_T$ with A. For $\bar{\beta}_T \sim 1/A^m$, m = 1;3/2;2 , A_m typically lies in the range $2 \lesssim A_m \lesssim 4.5$, A_m decreasing with m. The maximum is thus generally attained in a range which is technically accessible.

For special examples the above results have been verified with the SISYFUS-T power plant model. This code, in addition, gives the behaviour of the power density or wall load in the vicinity of the maximum. In the range $2 \lesssim A \lesssim 4.5$ p_f and q_w do not decrease more than roughly 50 % below their maximum value.

By means of this model the quantitative effect of finite burn times has been found to be modest. These calculations were based on the trapped-ion transport model. However, it is easy to see that the result is independent of the respective transport law, provided that $\tau_b >> \tau_o$ holds.

Our results, of course, permit no direct application to power plant overall optimization. But since maximum wall load implies maximum neutron yield they are of interest for the layout of future experimental devices.

Finally, it is worth noting that for $\bar{\beta}_T \sim 1/A$, which is widely accepted as the most probable scaling law, A_m typically lies in the range of 4. Our conclusions thus support the trend to higher aspect ratios in more recent designs.

ACKNOWLEDGEMENT

The authors gratefully acknowledge the helpful discussion of the layout constraints of superconducting magnets by M. Soell and the programming work and the performance of the numerical calculations by H. Gorenflo.

5. REFERENCES

/1/ Borrass, K.: Scaling of the Mean Fusion Power Density in Wall Contaminated Tokamak Reactors with Finite Burn Time. Third Topical Meeting on the Technology of Controlled Nuclear Fusion, Santa Fé, New Mexico, 1978.

/2/ Borrass, K.: A Zero-Dimensional Tokamak Transport Model. Part I, Max-Planck-Institut für Plasmaphysik Report, IPP 4/146, 1977.

/3/ Raeder, J.: Energy Balance of Fusion Power Plants as the Basis of System Studies. Max-Planck-Institut für Plasmaphysik Report, IPP 4/166, 1977.

/4/ Soell, M.: Maximum attainable Toroidal Magnetic Field for Tokamaks. Proc. of the Appl. Supercond. Conf., Pittsburgh, 1978.

/5/ Borrass, K., Buende, R., Daenner, W.: First Results with the SISYFUS Code. Third Topical Meeting on the Technology of Controlled Thermonuclear Fusion, Santa Fé, New Mexico, 1978.

/6/ Borrass, K., Buende, R. Daenner, W.: SISYFUS - A Simulation Model for Systematic Analyses of Fusion Power Plants. 10th Symposium on Fusion Technology, Padua, Italy, 1978.

APPENDIX

The maximum field obtainable at the inner coil is either determined by the critical field B_c, this being a material constant, or by some maximum strain, depending on the coil geometry, too. The latter dependence has been studied in Ref. /4/. The following expression for B_{max} is given there:

$$B_{max} \sim \sqrt{\frac{(2\pi\, r_1 - n\ell)\, b}{(r_1 + b/2)^2\, K}} \quad , \quad K = \frac{1}{2}\, \ell n\, \frac{r_2}{r_1} \; . \tag{1}$$

Here n is the number of coils and ℓ the gap between two inner legs. All other important quantities appearing in eq. (1) are explained by Fig. 6.

Instead of r_1, r_2, a we introduce A,f,V as new variables. We then get with

$$r_1 = R\text{-}a\text{-}\Delta = (A\text{-}1)\; a\text{-}\Delta$$

and

$$r_2 = R\text{+}a\text{+}\Delta = (A\text{+}1)\; a\text{+}\Delta$$

$$K = \frac{1}{2}\, \ell n\, \frac{r_2}{r_1} = \frac{1}{2}\, \ell n\, \left(\frac{A\text{+}1\text{+}f\text{-}1}{A\text{-}1\text{+}1\text{-}f}\right) = \frac{1}{2}\, \ell n\, \left(\frac{1+\frac{f}{A}}{1-\frac{f}{A}}\right) \approx \frac{f}{A} \; . \tag{2}$$

Hence

$$B_{max} \sim \sqrt{\frac{(2\pi\, r_1 - n\ell)b}{(r_1 + b/2)^2\, K}} \approx \sqrt{\frac{2\pi\, [(A\text{-}1)\; a\text{-}\Delta]\text{-}n\ell}{[(A\text{-}1)\; a\text{-}\Delta\, \text{+}b/2]^2}\, \frac{bA}{f}} =$$

$$\sqrt{\frac{2\pi\, \left(A\text{-}1\text{+}1\text{-}f\, -\, \frac{n\ell}{2\, a}\right)}{(A\text{-}1\text{+}1\text{-}f\text{+}b/2a)^2}\, \frac{pA}{af}} \; . \tag{3}$$

Assuming $\frac{n\ell}{2\pi a} << 1$ and $b/2a << 1$, we have

$$B_{max} \sim \sqrt{\frac{A}{(A\text{-}f)\; a\; f}} \; . \tag{4}$$

With $a \sim (V/A)^{1/3}$ we get, furthermore,

$$B_{max} \sim \frac{1}{f^{1/2}\,(1-f/A)^{1/2}} \left(\frac{A}{V}\right)^{1/6} . \qquad (5)$$

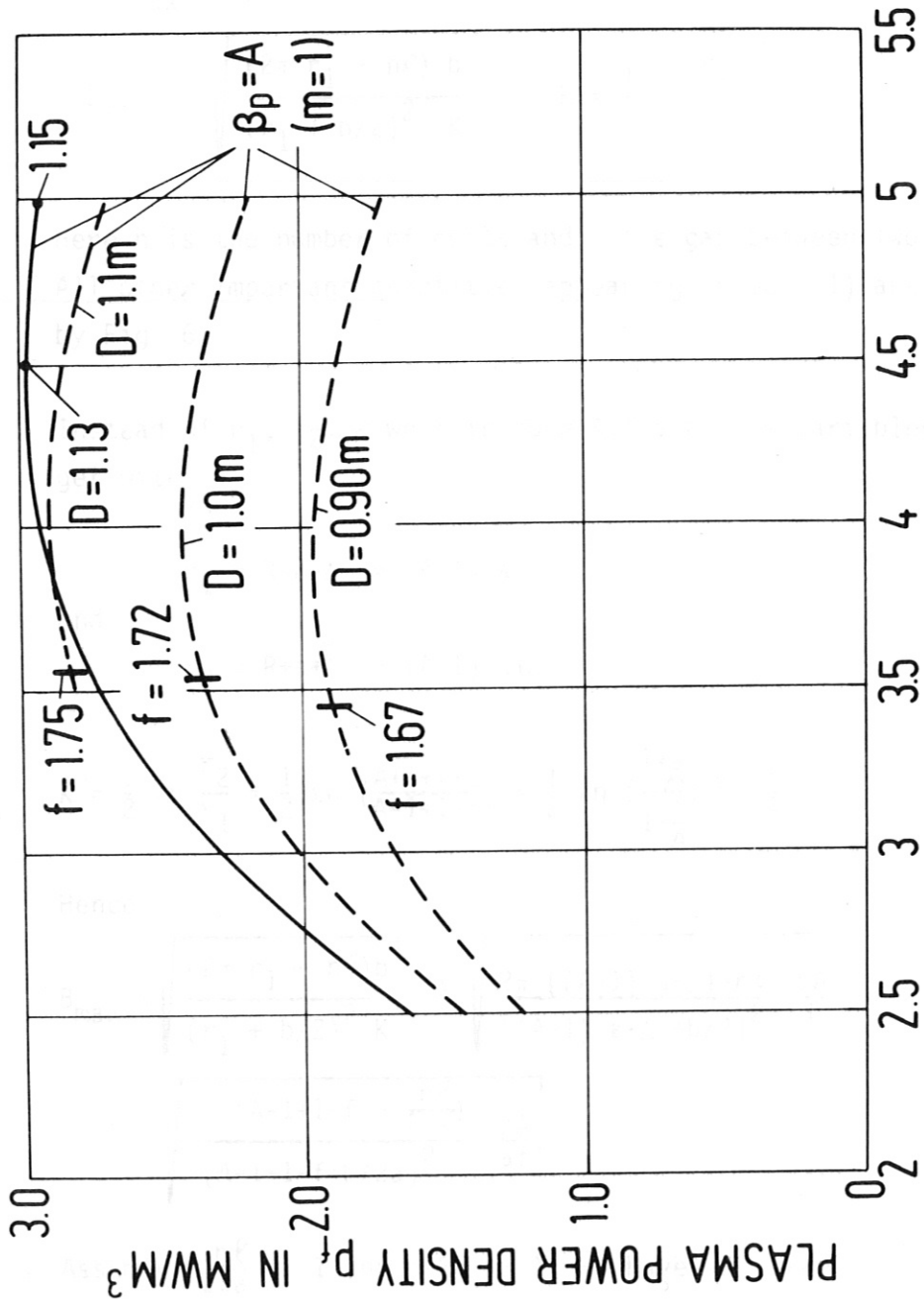

Fig. 1 Plasma power density p_f (cycle time average) as a function of the aspect ratio A ($P_{e,net}$ = 1500 MWe; τ_o = 50 s; anomalous outward diffusion of α-particles; impurity reflux coefficient γ = 0; D = thickness of the toroidal magnets; $\beta_p = A^{2-m}$; for definition of f see eq. (3); ▮ = maximum value according to eq. (20)).

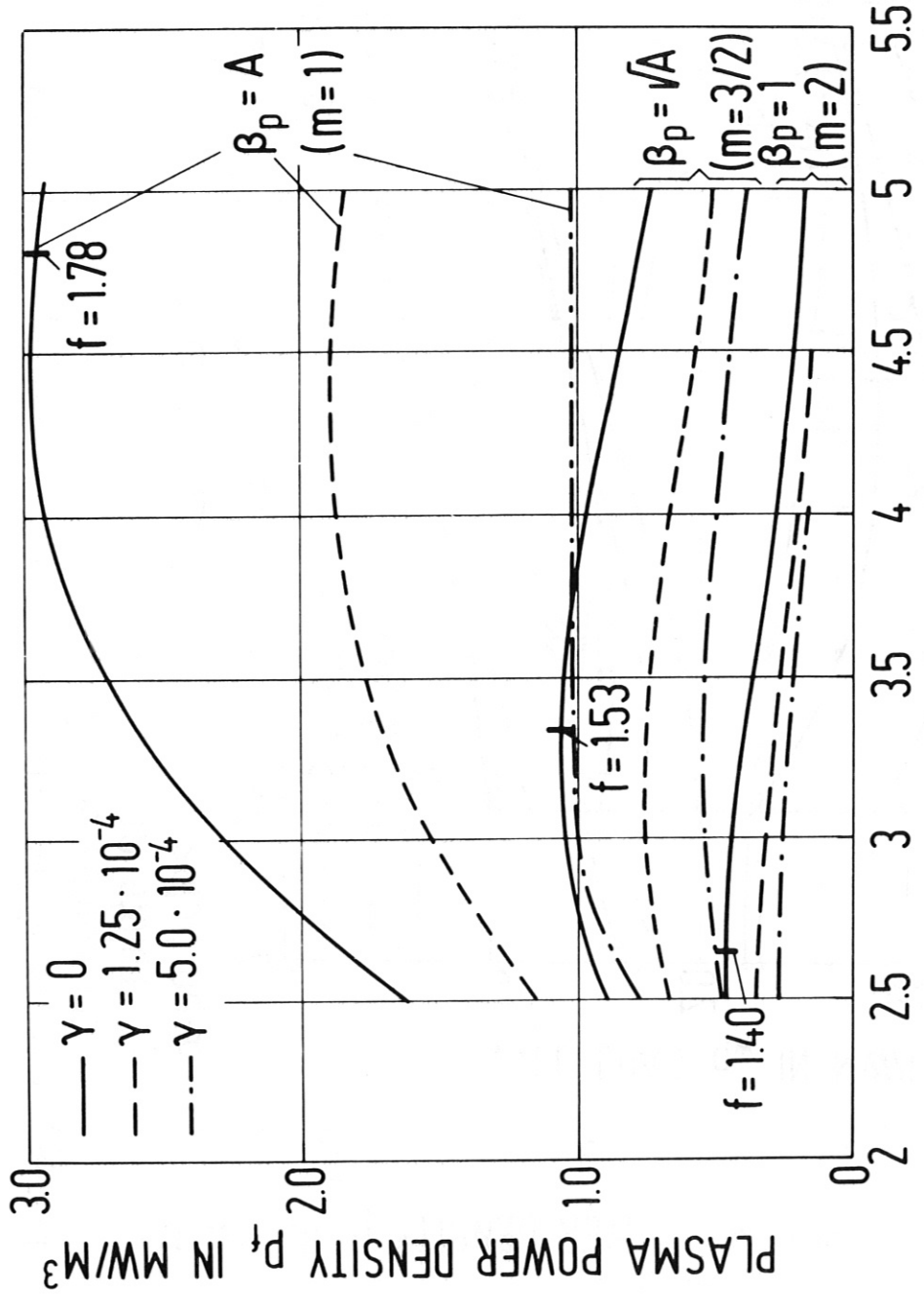

Fig. 2 Plasma power density p_f (cycle time average) as a function of the aspect ratio A ($P_{e,net}$ = 1500 MWe; τ_o = 50 s; anomalous outward diffusion of α-particles; γ = impurity reflux coefficient; $\beta_p = A^{2-m}$; for definition of f see eq. (3); ▌ = maximum value according to eq. (20)).

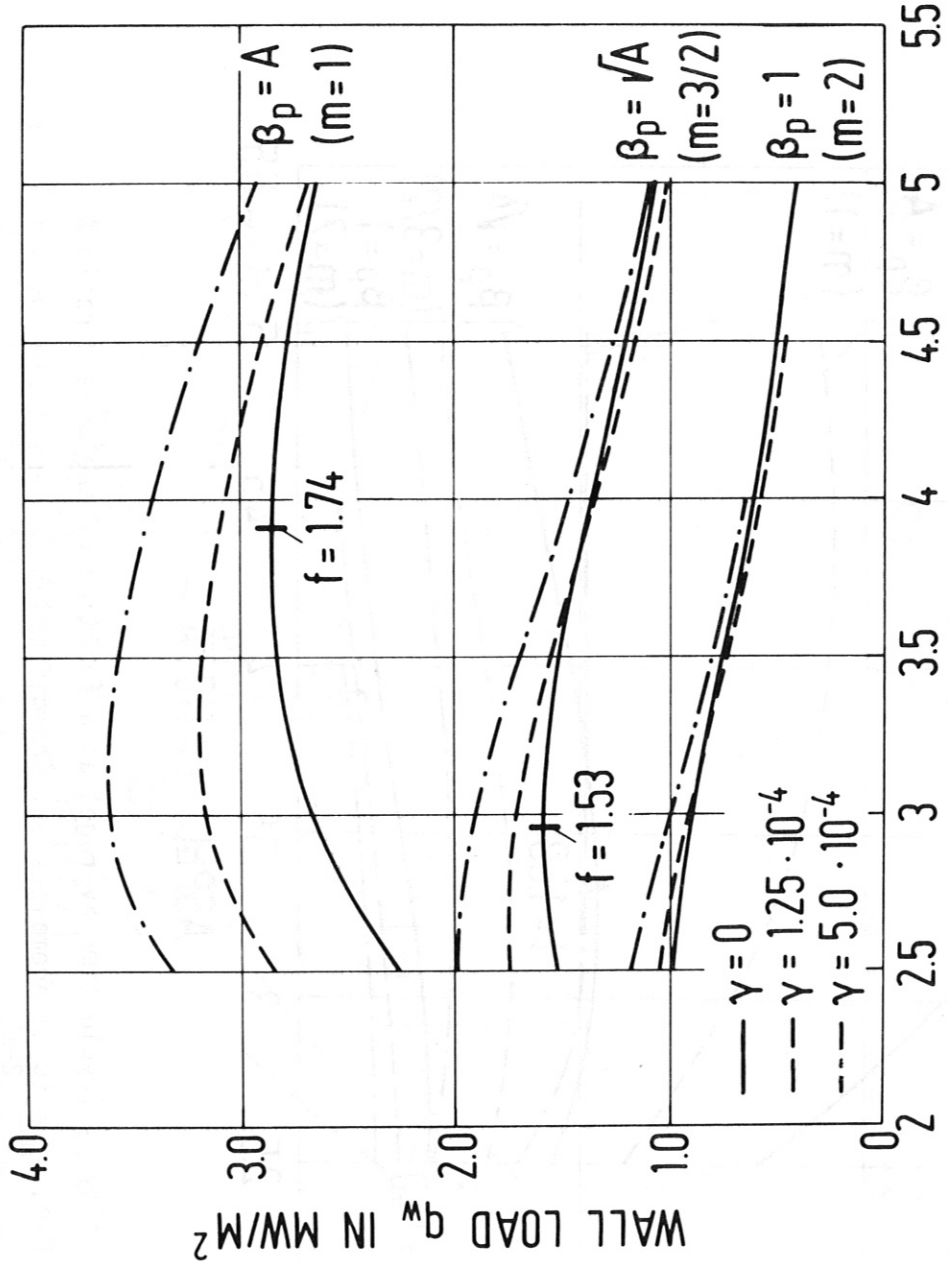

Fig. 3 Wall load q_w (burn time average) as a function of the aspect ratio A (same legend as Fig. 2)

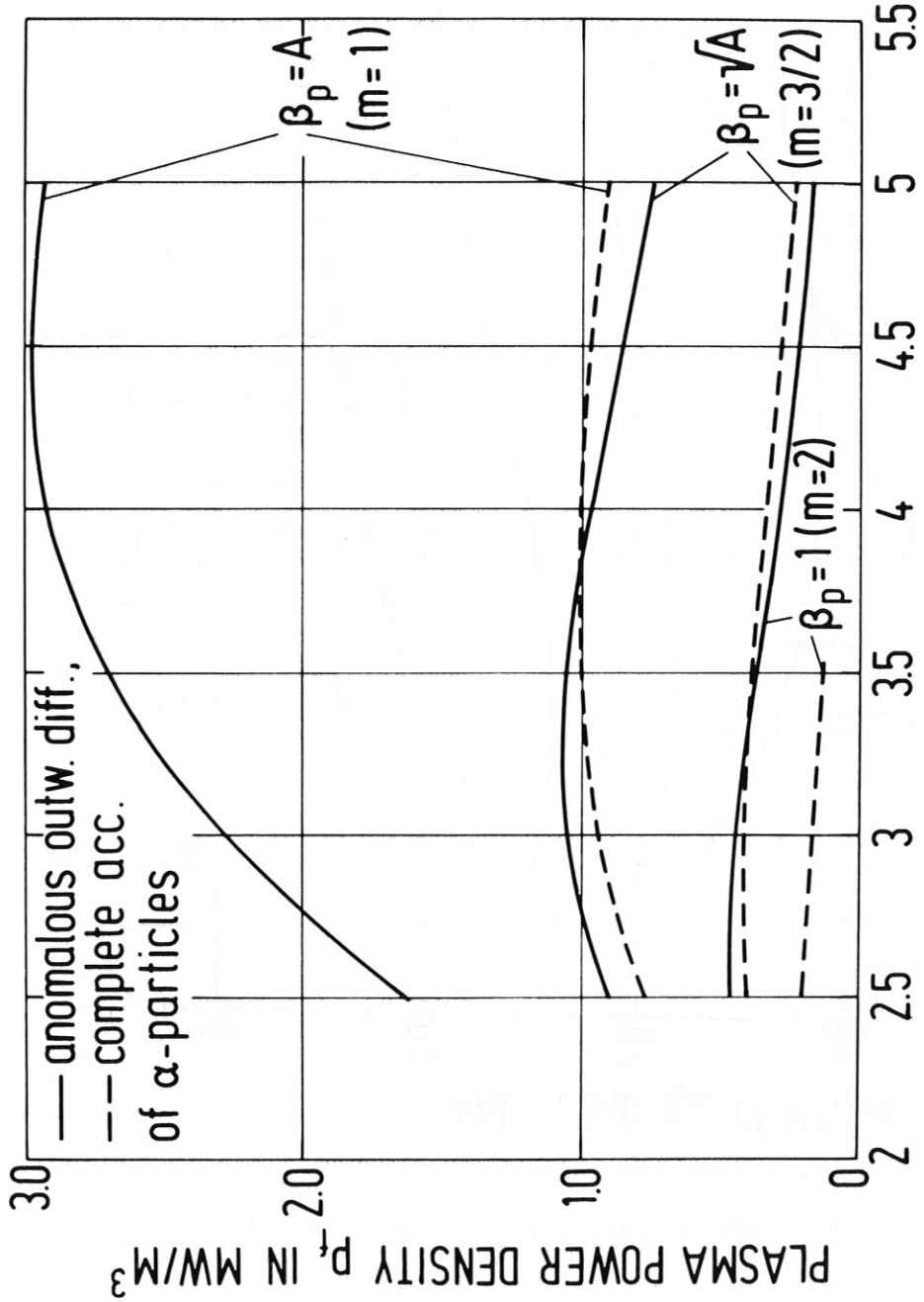

Fig. 4 Plasma power density (cycle time average) as a function of the aspect ratio A.
($P_{e,net}$ = 1500 MWe; τ_o = 50 s; impurity reflux coefficient γ = 0; $\beta_p = A^{2-m}$)

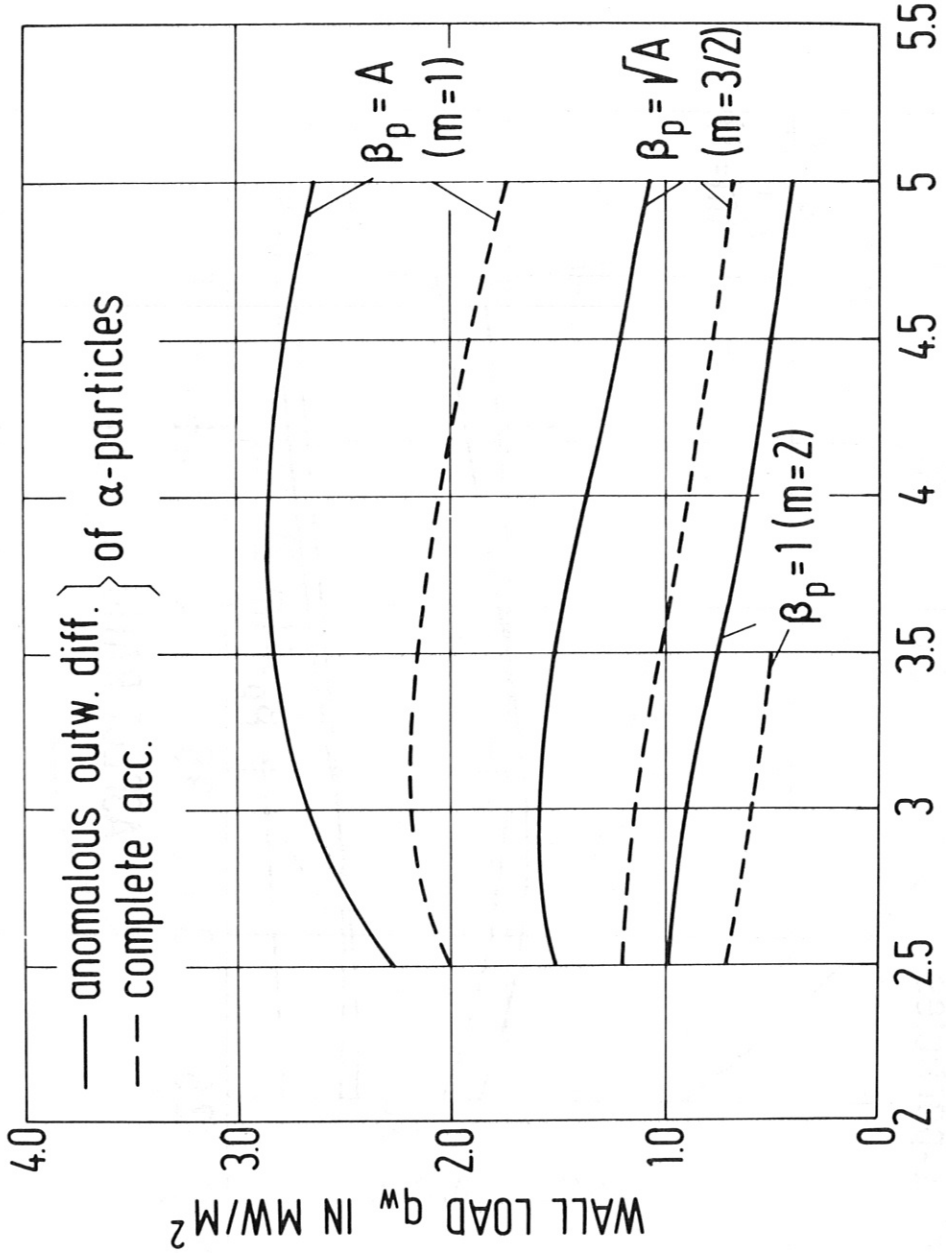

Fig. 5 Wall load q_w (burn time average) as a function of the aspect ratio A (same legend as Fig. 4)

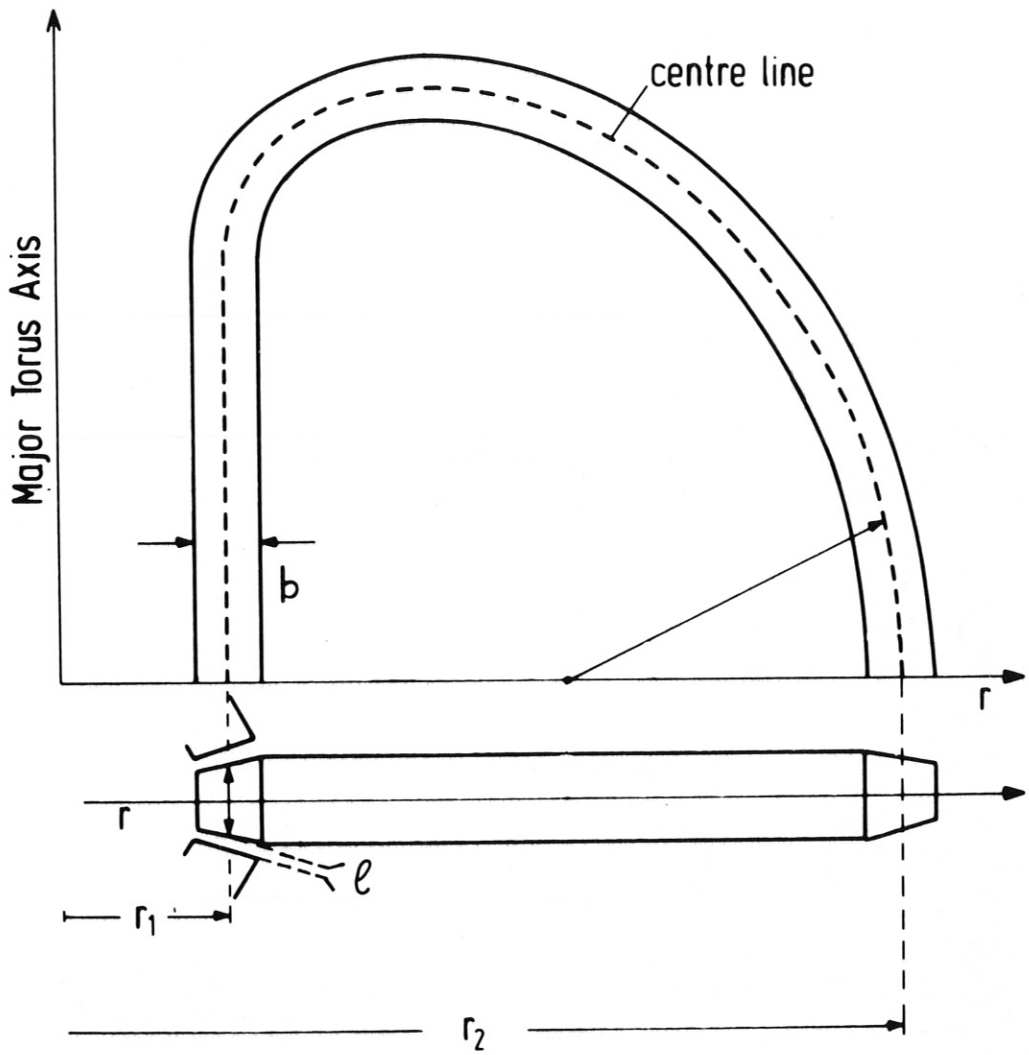

Fig. 6 Visualization of notations used in the Appendix